Two distinct ballistic processes in graphene

M. Lewkowicz,[1] B. Rosenstein,[2, 3, 1, *] and D. Nghiem[2]

[1] *Physics Department, Ariel University Center of Samaria, Ariel 40700, Israel*
[2] *Electrophysics Department, National Chiao Tung University, Hsinchu 30050, Taiwan, R. O. C.*
[3] *National Center for Theoretical Sciences, Hsinchu 30043, Taiwan, R. O. C.*

(Dated: July 19, 2011)

A dynamical approach to ballistic transport in mesoscopic graphene samples of finite length L and contact potential difference with leads U is developed. It is shown that at ballistic times shorter than both relevant time scales, $t_L = L/v_g$ (v_g - Fermi velocity) and $t_U = \hbar/(eU)$, the major effect of electric field is to creates the electron - hole pairs, namely causes interband transitions. At ballistic times lager than the two scales the mechanism is very different. The conductivity has its "nonrelativistic" or intraband value equal to the one obtained within the Landauer-Butticker approach for the barrier U resulting from evanescent waves tunneling through the barrier.

PACS numbers: 72.80.Vp 73.20.Mf 12.20.-m

I. INTRODUCTION

Electronic mobility in graphene, especially one suspended on leads, is extremely large [1], so that a graphene sheet is one of the purest electronic systems with the transport being considered ballistic [2, 3]. The ballistic flight time in these samples can be estimated as

$$t_L = L/v_g\,, \tag{1}$$

where $v_g \simeq 10^6 m/s$ is the graphene velocity characterizing the massless "ultrarelativistic" spectrum of graphene near Dirac points, $\varepsilon_k = v_g\,|\mathbf{k}|$, and L is the length of the sample that can exceed several μm [4]. The extraordinary physics appears right at the Dirac point at which the density of states vanishes. At this point graphene exhibits a quasi - Ohmic behaviour, $\mathbf{J} = \sigma\mathbf{E}$, even in the purely ballistic regime.

Determination of the value of the minimal DC conductivity at Dirac point in the limit of zero temperature has undergone a period of experimental and theoretical uncertainty. Several different values for the DC conductivity appeared. The value

$$\sigma_1 = \frac{4}{\pi}\frac{e^2}{h} \tag{2}$$

had been considered as the "standard" one for several years [6, 7] and appeared as a zero disorder limit of the self-consistent harmonic approximation [8]. It was derived for the *infinite* sample and this implies the assumption that the potential difference U at the contacts between the metallic leads and the graphene flake is unimportant. An alternative and independent approach to ballistic transport in mesoscopic graphene samples of *finite* length L [14] with a large contact barrier U was pioneered in [15] following ideas in [16]. They applied the Landauer - Büttiker formula for conductance derived for transport in (quasi) one-dimensional channels.

The value

$$\sigma_2 = \frac{\pi}{2}\frac{e^2}{h} \tag{3}$$

was obtained in the dynamical approach to an infinite sample [17] and is equal to the AC value calculated under the condition $\omega >> T/\hbar$ at finite temperatures [18–20]. The ballistic evolution of the current density in time after a sudden or gradual switching on of the electric field E was evaluated and approaches the large times limit $\sigma_2 E$. The electric field creates electron - hole excitations in the vicinity of the Dirac points similar to the Landau - Zener tunneling effect in narrow gap semiconductors [23]. Importantly, in graphene the energy gap is zero, thus the pair creation is possible at zero temperature and arbitrary small $\mathbf{E}$, *even within linear response*. Although the absolute value of the quasiparticle velocity v_g cannot be altered by the electric field due to the "ultrarelativistic" dispersion relation**,** the orientation of the velocity can be influenced by the applied field. The electric current, $e\mathbf{v}$, proportional to the projection of the velocity $\mathbf{v}$ onto the direction of the electric field is increased by the field. These two sources of current, namely creation of moving charges by the electric field (polarization) and their reorientation (acceleration) are responsible for the creation of a stable current [17, 22, 26]. The result within linear response is that the current settles very fast, on the microscopic time scale of $t_\gamma = \hbar/\gamma \simeq 0.24\ fs$ (γ being the hopping energy), on the asymptotic value.

A deeper analysis of the "quasi - Ohmic" graphene system beyond the leading order in perturbation theory in electric field revealed [27] that on the time scale

$$t_{nl} = \sqrt{\frac{\hbar}{eEv_g}}, \tag{4}$$

the linear response breaks down due to intensive Landau-Zener-Schwinger's (LZS) pair creation [28]. At times larger than t_{nl} the result is consistent with the WKB

approximation [26, 29]. This is in contrast to dissipative systems, in which the linear response limit can be taken directly at infinite time. This perhaps is the origin of the "regularization" ambiguities in graphene, since large time and small field limits are different.

In contrast, the Landauer - Büttiker (LB) approach hinges on the description of the leads in terms of a potential barrier of a certain non-zero barrier height $U(r)$ [10]. The barrier potential provides an additional time scale

$$t_U = \hbar/U. \tag{5}$$

In this note we rigorously apply the dynamical approach to study transport in mesoscopic samples. We demonstrate that the physics behind the two values of the DC conductivity is quite different despite the fact that numerically $\sigma_2 = 1.57e^2/h$ is just 24% higher than $\sigma_1 = 1.27e^2/h$ for the stripe geometry. These two physical processes governing the ballistic transport are quite distinct. One is fast and homogeneous: the interband channel, namely the electron - hole creation, sometimes referred to as Landau - Zener tunneling, or, in particle physics, the Schwinger's pair creation[35]. It is unique to graphene and has certain surprising features. For example, this channel of conduction "dries out" or is depleted for any finite sample. The second mechanism, the intraband transition, despite constituting a peculiar "relativistic" kind of electron acceleration, is much more common. It is important for transport only for a sufficiently large contact potential between the leads and the graphene sample and unlike the interband channel, is a long time phenomenon.

We use the dynamical approach to determine what process is dominant for the evolution of the I-V curve of a finite graphene sample directly at the neutrality point, with the contact barrier taken into account. The physics depends essentially on the relation of a time scale t with respect to the three physical time scales t_L, t_U and t_{nl}. The analysis (the details of the calculation are given in [34]) shows that for a finite barrier potential and finite length the infinite time limit coincides in linear response with a generalization of the LB calculation in [15].

II. SMALL CONTACT BARRIER: DYNAMICAL APPROACH TO THE ELECTRON - HOLE CHANNEL OF THE BALLISTIC TRANSPORT

A. The infinite sample

The electron - hole channel in the infinite sample was analyzed in [17] employing the "first quantized" Hamiltonian

$$H = -i\boldsymbol{\sigma}\cdot\left(\boldsymbol{\nabla}+\frac{e}{c}\mathbf{A}\right). \tag{6}$$

$\mathbf{A} = (0, -cEt)$ is the vector potential describing the electric field which is switched on at $t = 0$, oriented along the y axis and, importantly, is coordinate independent. We employ units in which $\hbar = v_g = 1$. In momentum basis, $\psi_{\mathbf{r}} = \frac{1}{\sqrt{WD}}\sum_{\mathbf{k}} e^{i\mathbf{k}\cdot\mathbf{r}}\psi_{\mathbf{k}}$, where D is an infrared cutoff and W is the width that also will be treated as large.

The spectrum before the electric field is switched on is divided into positive and negative energy parts describing the valence and conduction band:

$$(\boldsymbol{\sigma}\cdot\mathbf{k})\,u_{\mathbf{k}} = -\varepsilon_{\mathbf{k}}u_{\mathbf{k}}; \qquad (\boldsymbol{\sigma}\cdot\mathbf{k})\,v_{\mathbf{k}} = \varepsilon_{\mathbf{k}}v_{\mathbf{k}}; \tag{7}$$

$$u_{\mathbf{k}} = \frac{1}{\sqrt{2}}\begin{pmatrix}1\\-z_{\mathbf{k}}\end{pmatrix}; \qquad v_{\mathbf{k}} = \frac{1}{\sqrt{2}}\begin{pmatrix}1\\z_{\mathbf{k}}\end{pmatrix}, \tag{8}$$

where $z_{\mathbf{k}} = (k_x + ik_y)/\varepsilon_{\mathbf{k}}$ is a phase and $\varepsilon_{\mathbf{k}} = |\mathbf{k}|$. The solution to the matrix Schrödinger equation in sublattice space $i\partial_t\psi_{\mathbf{k}} = \boldsymbol{\sigma}\cdot\left(\mathbf{k}+\frac{e}{c}\mathbf{A}\right)\psi_{\mathbf{k}}$ is is a "spinor" in the sublattice space

$$\psi_{\mathbf{k}}(t) = \begin{pmatrix}\psi^1_{\mathbf{k}}(t)\\ \psi^2_{\mathbf{k}}(t)\end{pmatrix}, \tag{9}$$

The initial condition corresponding to a second quantized state at zero temperature in which all the negative energy states are occupied and all the positive energy states are empty is $\psi_{\mathbf{k}}(t=0) = u_{\mathbf{k}}$.

The evolution of the current density, $\hat{\mathbf{J}} = -4e\hat{\psi}^\dagger_r\boldsymbol{\sigma}\hat{\psi}_r$ of a state in terms of this amplitude is

$$j_y(t) = -4e\sum_{\mathbf{k}:\boldsymbol{\varepsilon}_{\mathbf{k}}<0}\psi^\dagger_{\mathbf{k}}(t)\,\sigma_y\psi_{\mathbf{k}}(t), \tag{10}$$

was calculated for arbitrary E in ref. [28]. The factor 4 is due to spin and valley degeneracies of the Weyl fermions. To leading order in the DC electric field one obtains [17] $\sigma = \sigma_2$, Eq.(3). Corrections to the conductivity were computed in [27] and reveal that the linear response breaks down at t_{nl} and is perhaps a source of the "regularization ambiguity" in linear response.

The simple method of calculation used here hinges on the translational invariance of both the sample and the electric field.

B. Linear response in a finite sample

To model the perturbing bias voltage we assume that electric field is homogeneous in the segment $-L/2 < y < L/2$, and therefore can be described by a scalar potential V, see the dashed line in Fig.1, (and $\mathbf{A} = 0$). The current, to leading order in perturbation V is:

$$I_y(t) = -4W\sum_{\mathbf{l},\mathbf{p}}\frac{1-e^{-i(\varepsilon_{\mathbf{p}}+\varepsilon_{\mathbf{l}})t}}{\varepsilon_{\mathbf{p}}+\varepsilon_{\mathbf{l}}}\langle u_{\mathbf{l}}|V|v_{\mathbf{p}}\rangle\langle v_{\mathbf{p}}|J_y|u_{\mathbf{l}}\rangle + cc. \tag{11}$$

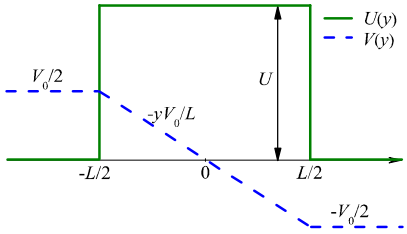

FIG. 1: Potential barrier U(y) (green line) describes contacts of a sample with leads, while the bias electric potential V(y) (blue dashed line) describes the nearly homogeneous applied electric sample.

As explained in detail in section IV of ref. [27], the current within the Weyl model has an ultraviolet divergence that should be removed in a chiral invariant manner. Since the present case is not different in this respect from the infinite range field, the details are omitted. After some algebra the conductivity (for large W so that continuum momentum can be used) takes the form

$$\sigma(t) = \frac{e^2}{\pi^3}\int_{k=-\infty}^{\infty}\int_{p,l=0}^{\infty} \frac{\sin\left[(p-l)L/2\right](l\varepsilon_{kp}-p\varepsilon_{kl})}{(p-l)^2\varepsilon_{kl}\varepsilon_{kp}}\frac{\sin\left[t\left(\varepsilon_{kp}+\varepsilon_{kl}\right)\right]}{\varepsilon_{kp}+\varepsilon_{kl}}, \quad (12)$$

where $k = l_x = p_x, l = l_y, p = p_y$. This function is given as the red line Fig.2a of ref.([34]). Before $t = t_L/2$, $\sigma(t) = e^2/4$, therefore in physical units one recovers the "dynamical" value $\sigma_2 = \frac{\pi}{2}\frac{e^2}{h} = \frac{e^2}{4\hbar}$.This is just the result of pseudo-relativistic invariance (maximal velocity v_g) of the Weyl model. The effect of the finite extent of the electric field has no time to propagate to the center of the sample where the current is defined. Then the current drops fast and settles at t_L into a power decrease

$$\sigma(t) = \sigma_2\frac{L}{\pi t}. \quad (13)$$

Until now the linear response approximation was used. Hence, for a finite range of the electric field (finite distance between the electrodes) a stationary flow state is only possible beyond linear response.

C. Electron-hole conductance beyond linear response

There are two characteristic times beyond linear response, t_L and t_{nl}. Analytic and numerical solutions of the tight binding model[28], as well as of the Dirac model describing the physics near the Dirac point demonstrated[26, 27] that at t_{nl} the creation of electron - hole pairs become dominant and is well described by an adaptation of the well - known (non-analytic in $\mathbf{E}$) Schwinger electron - positron pair creation rate $\frac{d}{dt}N \propto (eE)^{3/2}$. The polarization current is $J(t) = -2ev_gN(t)$ and therefore Schwinger's creation rate at asymptotically long times leads to a linear increase with time: $\sigma(t) = \sigma_2(eE)^{1/2}t$. The physics of pair creation is highly non-perturbative and non-linear in nature. The rate can be intuitively understood using the much simpler instanton approach[25, 26].

Adaptation of the instanton approach to finite length sample is quite cumbersome, however the long time limit is simple, as was shown in ref.[30]. The result for the conductivity is presented for the possibilities $t_L >> t_{nl}$, $t_L << t_{nl}$ or $t_L \sim t_{nl}$ in Fig. 2 of ref.[34].

III. CONTACT BARRIER: STATIONARY PROPERTIES AND THE LANDAUER - BÜTTIKER APPROACH.

A. Phenomenological description of contacts. Symmetry of the Hamiltonian.

One models the effect of coupling to leads by a finite (and sometimes very large [15]) potential energy barrier. The simplest model is the square barrier, see Fig.1.

The "first quantized" operator H_{1Q} now contains the barrier potential $U(y)$:

$$H_{1Q} = -i\sigma\cdot\nabla + U(y). \quad (14)$$

The barrier breaks the translational symmetry, however, for the simple form of the symmetric barrier we adopted the operator H_{1Q} is invariant under reflection, $P: y \to -y$, *supplemented by the spinor rotation*,

$$S = P\sigma_x, \qquad [H_{1Q}, S] = 0. \quad (15)$$

B. T - matrix

The LB approach utilizes the notion of a transmission coefficient through the channel n, $T_n \equiv |t_n|^2$, where t_n is its amplitude [23]. The conductance is

$$G = \frac{e^2}{h}\sum_n T_n. \quad (16)$$

Therefore one should solve the "classical" Weyl equation with a barrier

$$H_{1Q}\psi = \left[-i\sigma\cdot\nabla + U(y)\right]\psi = \varepsilon\psi. \quad (17)$$

With periodic boundary conditions the momentum in the direction perpendicular to the field is $p_x \equiv k = \frac{2\pi}{W}n_x$. Despite the lack translational symmetry in the field direction y due to the barrier, one can still use the momentum $p_y \equiv p$ as a good quantum number for scattering

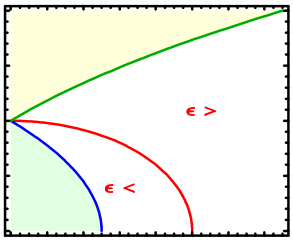

FIG. 2: Kinematics of scattering states of the first quantized Weyl equation with potential barrier. The red line corresponds to $p, l = \sqrt{U^2 - k^2}$, the green to $p, l = \sqrt{U(U+2k)}$, and the blue to $p, l = \sqrt{U(U-2k)}$. The lines separate kinematical regions for the intraband transitions. Here $U = 1$.

states. The sign of energy determines the wave function in the leads, namely distinguishes between the u and the v spinors. The reflection symmetry converts left movers into right movers

$$Sv_{k,p}e^{ipy} = z_p v_{k,-p}e^{-ipy}; \quad Su_{k,p}e^{ipy} = -z_p u_{k,-p}e^{-ipy}. \tag{18}$$

where we suppressed the index k in $z_{kp} = (k+ip)/\varepsilon_{\mathbf{k}}$.

The "out of barrier" equation is just the free Weyl equation with negative and positive energy solutions, $\psi = u_{kp}e^{i(kx+py)}$ (hole) and $\psi = v_{kp}e^{i(kx+py)}$ (electron). It should be matched with the "in barrier" solution. Several distinct kinematic possibilities exist which are summarized in Fig.2.

1. Energies above the barrier, $\varepsilon > U$. Both inside and outside one has electron v- states with different momenta. Outside the barrier $p = \sqrt{\varepsilon^2 - k^2}$, while inside the barrier the momentum in the field direction is

$$q = \sqrt{(\varepsilon - U)^2 - k^2}. \tag{19}$$

One has a wave (real q) inside for $p > p_2 \equiv \sqrt{(U + 2|k|)U}$, while there is an evanescent particle state inside for $\sqrt{U^2 - k^2} \equiv p_U(k) < p < p_2$.

2. Positive energy states below the barrier, $0 < \varepsilon < U$. One has the v spinor (electron) outside the barrier, while the u spinor (hole) inside. For momenta p in the range

$$\sqrt{(U - 2|k|)U} \equiv p_1 < p < p_U, \tag{20}$$

the states are evanescent hole states. At yet lower energies, $p < p_1$, one has a propagating state, but this time a *hole*. This relativistic feature is the cause of the Klein paradox.

3. Negative energy states, $\varepsilon < 0$. Outside the barrier now one has $\varepsilon = -\sqrt{p^2 + k^2}$. This is another purely "relativistic" possibility in which one has holes both outside and hence inside the barrier.

The Schrödinger equation above the barrier $\varepsilon > U$ is solved by the scattering states for right movers, $p > 0$,

$$\phi_{kp}(y) = \frac{1}{\sqrt{DW}} \begin{cases} v_{kp}e^{ipy} + r_{kp}v_{k,-p}e^{-ipy}; & y < -L/2 \\ A_{kp}v_{kq}e^{iqy} + B_{kp}v_{k,-q}e^{-iqy}; & -L/2 < y < L/2 \\ t_{kp}v_{kp}e^{ipy}; & L/2 < y \end{cases}. \tag{21}$$

which together with the matching conditions determine the T-matrix and are easily solved. The electron v states have to be replaced with u states in the case of a hole, so in the second energy region in the barrier part $v \to u$, while in the third energy region in all parts $v \to u$. For example, for evanescent modes below the barrier one obtains

$$t_{kp} = \frac{\left(z_p^2 - 1\right)\left(z_q^2 - 1\right)}{e^{-iqL}\left(1 - z_p z_q\right)^2 - e^{iqL}\left(z_p - z_q\right)^2}. \tag{22}$$

Let us first consider, following ref.[15], only evanescent states contributions under the barrier. Substituting the transmission coefficient of Eq.(22), one obtains the following limiting value of conductivity for a large barrier "strength" $UL \equiv \Omega = t_L/t_U$:

$$\sigma_{LB}(\Omega >> 1) = \frac{2e^2\Omega}{\pi^2}\int_{k=0}^{U} \cosh^{-2}(kL) = \frac{2e^2}{\pi^2} = \sigma_1. \tag{23}$$

One therefore can apply the dynamical approach to try to understand the crossover from the short ballistic time, the electron - hole "bulk" dynamics, to the long ballistic time, the barrier reflection dominated dynamics.

IV. EVOLUTION OF THE CURRENT IN GRAPHENE WITH BARRIER

A. The current in linear response

In linear response one obtains two contributions with completely different physical interpretations. In the first term the summation is over electron states above $\mu = U$ (in this note $U_{gate} = 0$) and electron states below the Fermi level,

$$I_{ee}(t) = -W\sum_k \sum_{p:\varepsilon_{kp}>U} \sum_{l:\varepsilon_{kl}<U} \frac{1 - e^{-i(\varepsilon_{kp}-\varepsilon_{kl})t}}{\varepsilon_{kp} - \varepsilon_{kl}} \mathcal{V}_{k,lp}^{++ST} j_{k,pl}^{++TS} + cc. \tag{24}$$

where $\mathcal{V}_{k,lp}^{++ST} = \int_y V(y)\,\phi_{kl}^{S\dagger}(y)\,\phi_{kp}^{T}(y)$ and $j_{k,pl}^{++TS} = -4e\phi_{kp}^{T\dagger}(y=0)\,\sigma_y\phi_{kl}^{S}(y=0)$. The summation over T, S, which denote symmetric and antisymmetric states, is understood. The second contribution sums over electrons above μ and all the hole states below.

$$I_{eh}(t) = -W \sum_{k,l} \sum_{p:\varepsilon_{kp}>U} \frac{1-e^{-i\left(\varepsilon_{kp}+\varepsilon_{kl}\right)t}}{\varepsilon_{kp}+\varepsilon_{kl}} \mathcal{V}_{k,lp}^{-+ST} j_{k,pl}^{+-TS} + cc. \quad (25)$$

where $\mathcal{V}_{k,lp}^{-+ST} = \int_y V(y)\, \varphi_{kl}^{S\dagger}(y)\, \phi_{kp}^{T}(y)$ and $j_{k,pl}^{+-TS} = -4e\phi_{kp}^{T\dagger}(0)\, \sigma_y \varphi_{kl}^{S}(0)$. The hole's momentum has no restriction since its energy is always negative. The first contribution is the "one-particle" type (the intraband channel), very much like in more common manybody electronic systems. The second contribution, to the contrary, is purely ultrarelativistic (the interband channel) and describes the electron-hole pair creation, very much like in the infinitely long flake discussed in Section II.

B. The intraband contribution

The one-particle (electron - electron) contribution to the conductivity is shown in Fig. 3 as red curves for various values of Ω as a function of time. At times shorter than both t_L and t_U it rises linearly, oscillates for $\Omega > 1$ and approaches the LB result.

Short time asymptotics

The short time limit of the electron - electron contribution to the conductivity leads to a small conductivity raising linearly shown in Fig. 3 (red lines). For the case $\Omega \lesssim 1$ ($t_L < t_U$), represented in Fig.3 by $\Omega = \pi/16$, $\pi/4$, the intraband contribution is positive and increases monotonically. However, when $\Omega > 1$ ($t_L > t_U$) represented in Fig.4 by $\Omega = \pi$, 2π, it becomes negative.

Long time asymptotics

Due to the oscillating functions in Eq.(25) the long time asymptotics is due solely to the region of the three dimensional integral when $\varepsilon_{kp} - \varepsilon_{kl} \to 0$. Consequently, in view of the discussion of the various kinematical regions in subsection III B, summarized in Fig.2, the limit is dominated by integrating over the transitions from evanescent states above the barrier (region 1) to evanescent states below the barrier (region 2). At large times $t > t_U$, one obtains

$$\sigma^{ee}(\Omega >> 1) = 4\frac{e^2\Omega}{\pi^3}\frac{\pi}{2}\int_{\bar{k}=0}^{1} \frac{1}{\cosh^2\left(\bar{k}\Omega\right)} = \frac{e^2}{2\pi}\frac{4}{\pi}. \quad (26)$$

This is one of the main results of the paper. The electron - electron contribution, starting from the dynamical approach, converges at large times to σ_1, Eq.(2).

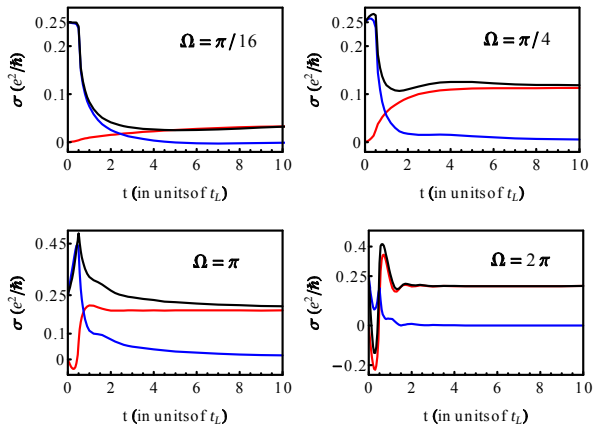

FIG. 3: Conductivity of finite length samples for $\Omega = UL/\hbar v_g = \pi/16, \pi/4, \pi, 2\pi$. The intraband contribution is the red line, interband contribution - blue lines. The total conductivity - the black lines. The time is given in units of $t_L = L/v_g$, while unit of conductivity is $e^2/\hbar$.

C. The interband contribution

The expression for conductivity $\sigma^{eh}(U, L, t)$ is UV divergent like the conductivity of the infinite sample biased in the region of length L that was studied in subsection II B (and which is solely due to the electron - hole pairs). Their difference $\Delta\sigma^{eh}$ however is finite. The results are given in Fig.3 for several Ω as blue lines. At small times it starts with the ultrarelativistic value $\sigma_2 = \frac{1}{4}\frac{e^2}{\hbar}$ and at relatively large times ($t_U >> t > t_L$) it decays as $\frac{1}{4\pi\bar{t}}$. This short time value σ_2 does not change when $U > 0$ provided the time is smaller than $t_L/2$. This follows from the fact that in relativistic graphene information about barrier cannot arrive at the center of the sample before that time. The long time behaviour of the electron - hole contribution is dominated, due to oscillations, by the region $\varepsilon_{kp} + \varepsilon_{kl} \to 0$.In this limit it is simple to calculate $\Delta\sigma^{eh}$ for special values of Ω. One can fit the long time asymptotics as $\Delta\sigma^{eh} \sim \cos(\Omega)/4\pi\bar{t}$.

V. DISCUSSION AND CONCLUSIONS

Two different kinds of ballistic behaviour occur in undoped graphene at zero temperature. One is a very unusual "ultra - relativistic" interband physics. Electron - hole pairs are copiously created via Landau-Zener-Schwinger's mechanism by an applied electric field. It is not dependent on leads and finite size effects of the graphene sample. To the contrary, the intraband physics is mostly sensitive to finite size effects and contacts. The first mechanism results within linear response in the universal bulk value σ_2 of conductivity, while the second is

characterized by a shape dependent linear response with the effective conductivity σ_1 for large aspect ratio rectangular flakes.

Now we recapitulate under what conditions either of these two processes is dominant in experiments on a time scale $1/\omega$ in an AC electric field E (or in a pulse of duration $1/\omega$) for a graphene flake of length L and a contact barrier potential U. Here we classify various practically important ranges of sample (U, L) and experimental (ω, E) parameters.

A. "Unintrusive" experiments, $U = 0$

In reflectance and transmission experiments in visible to mid IR or even microwave range [40] there are no leads, hence no potential barrier, $U = 0$. The interband (Landau - Zener - Schwinger) process is dominant for any practically length and electric field E. However, the transport can be either linear or highly nonlinear.

(i) For $1/\omega < t_{nl} = \sqrt{\hbar/eEv_g}$ one has linear response, $J = \sigma_2 E$, with the interband value of conductivity $\sigma_2 = \frac{\pi}{2}\frac{e^2}{h}$. In this case the nonlinear Schwinger's pair creation regime is not yet reached.

(ii) For $1/\omega > t_{nl}$ *and* $t_{nl} < t_L = L/v_g$ the transport is still dominated by electron - hole channel, but is nonlinear. The electron - hole pairs are efficiently created due to the LZS mechanism with rate proportional to $E^{3/2}$. This results in the I - V curve

$$J = \frac{eL}{\pi^2}\left(\frac{eE}{\hbar}\right)^{3/2}. \tag{27}$$

(iii) For $1/\omega > t_{nl}$ *and* $t_{nl} > t_L$ the transport is still dominated by electron - hole channel and the LZS process but since the electric field is applied in the limited space (length L which is not large enough) and the current is much smaller:

$$J = \frac{2eL^2}{\pi^2 v_g}\left(\frac{eE}{\hbar}\right)^2. \tag{28}$$

B. Large barrier

In samples on substrate with metallic leads the work function of the graphene and the metal is typically different and as a result the contact potential difference is of order $U = 0.1 - 1eV$, see calculations in [13] and references therein. In this case the corresponding time scale $t_U = \hbar/U < 7fs$ and typically smaller than any of the other scales $t_L = L/v_g, t_{nl} = \sqrt{\hbar/eEv_g}$. This leads to an effective suppression of the electron - hole channel for all the frequencies in the infrared range and smaller (including DC) and the physics is dominated by the electron - electron channel.

(i) $1/\omega > t_U$. The DC conductance is given by the Landauer - Bütticker formula and is more sensitive to the properties of the leads than those of graphene. When graphene is "nominally" at Dirac point, namely, when the chemical potential of the lead is on the barrier, graphene is still contaminated by charges tunneling into the stripe from the leads. These electrons are accelerated and lead to the mesoscopic type of conductance. For a large aspect ratio the effective conductivity is $\sigma_1 = \frac{4}{\pi}\frac{e^2}{h}$. The assumption of an "infinite" barrier was made early on in [15] in order to develop the mesoscopic approach to transport in graphene.

(ii) $1/\omega < t_U$. The high frequencies (microwave and above) experiments are done without leads. However if one had a set-up with leads it could not significantly alter the pseudo-Ohmic behaviour with $\sigma = \sigma_2$ since the contaminated regions constitute only a small fraction of the sample. There is no effect of ballistic acceleration across the sample for large frequencies or short pulses.

* Electronic address: vortexbar@yahoo.com

[1] Morozov S V *et al* 2008 *Phys. Rev. Lett.* **100** 016602
[2] Du X *et al* 2008 *Nature Nanotechnology* **3** 491
[3] Bolotin K I *et al* 2008 *Phys. Rev. Lett.* **101** 096802
[4] Andrei E Y, Talk at Workshop on Nonequilibrium Phenomana, Kanpur, January 2010.
[5] Novoselov K S *et al* 2005 *Nature* **438**, 197 ; Zhang Y *et al* 2005 *Nature* **438** 201
[6] Castro Neto A H *et al* 2009 *Rev. Mod. Phys.* **81** 109 ; Peres N M R 2010 *Rev. Mod. Phys.* **82** 2673
[7] Fradkin E 1986 *Phys. Rev. B* **33** 3263; Ludwig A W W *et al* 1994 *Phys. Rev. B* **50** 7526; Gusynin V P and Sharapov S G 2006 *Phys. Rev. B* **73** 245411; Ryu S *et al* 2007 *Phys. Rev. B* **75**, 205344 ; Cserti J 2007 *Phys. Rev. B* **75** 033405
[8] It was noted by Ziegler, Ziegler K 2006 *Phys. Rev. Lett.* **97** 266802 ; 2007 *Phys. Rev. B* **75**, 233407 that different regularizations within the Kubo formalism resulted in different values of the DC conductivity.
[9] Xia F *et al* 2011 *Nature Nanotechnology* **6** 179 ; Du X *et al* 2008 *Nature Nanotechnology* **3** 491
[10] Do V N and Dollfus P 2009 *J. Appl. Phys.* **106** 023719; 2010 *J. Phys. Cond. Mat.* **22** 425301
[11] Schomerus H 2007 *Phys. Rev. B* **76** 045433; Robinson J P and Schomerus H 2007 *Phys. Rev. B* **76** 115430 ; Blanter Y M and Martin I 2007 *Phys. Rev. B* **76** 155433
[12] R. Golizadeh-Mojarad and S. Datta 2009 *Phys. Rev. B* **79** 085410
[13] Khomyakov P A *et al* 2010 *Phys. Rev. B* **82** 115437
[14] Donneau R *et al* 2008 *Phys. Rev. Lett.* **100** 196802
[15] Tworzydło J *et al* 2006 *Phys. Rev. Lett.* **96** 246802
[16] Katsnelson M I 2006 *Eur. Phys. J. B* **51** 157
[17] Lewkowicz M and Rosenstein B 2009 *Phys. Rev. Lett.* **102** 106802

[18] T. Ando, Y. Cheng and H. Suzuura, *J. Phys. Soc. Jap.* **71**, 1318 (2002); N.M.R. Peres, F. Guinea and A. H. Castro Neto, *Phys. Rev. B* **73**, 125411 (2006).
[19] Falkovsky L A and Varlamov A A 2007 *Eur. Phys. J.* B **56** 281
[20] Gusynin V P *et al* 2007 *Phys. Rev. Lett.* **98** 157402; Min H and MacDinald A H 2009 *Phys. Rev. Lett.* **103** 067402
[21] Beneventano *et al* 2009 *J. Phys. A* **42** 275401
[22] Fritz L *et al* 2008 *Phys. Rev.* B **78** 085416
[23] Davies J H 1998 *The Physics of Low-dimensional Semiconductors: An Introduction*, Cambridge Univesity Press, New York
[24] Gavrilov S P and Gitman D M 1996 *Phys. Rev. D* **53** 7162 ; Kim S P and Page D N 2002 *Phys. Rev. D* **65** 105002
[25] Casher A *et al* 1979 *Phys. Rev.* D **20** 179
[26] Dora B and Moessner R 2010 *Phys. Rev. B* **81** 165431
[27] Kao H C *et al* 2010 *Phys. Rev.* B **81**
[28] Rosenstein B *et al* 2010 *Phys. Rev. B* **81** 041416(R)
[29] Allor D *et al* 2008 *Phys. Rev. D* **78** 096009 ; Cohen T D and McGady D A 2008 *Phys. Rev. D* **78** 036008
[30] Barreiro A *et al* 2009 *Phys. Rev. Lett.* **103** 076601; Vandecasteele N *et al* 2010 *Phys. Rev.* B **82** 045416
[31] E.B. Sonin, *Phys. Rev. B* **77**, 233408 (2008); *Phys. Rev. B* **79**, 195438 (2009).
[32] Rycerz A *et al* 2010 *Phys. Rev. B* **80** 125417
[33] Perfetto E *et al* 2010 *Phys. Rev. B* **82** 035446
[34] Lewkowicz M *et al* arXiv:1107.3039v1 [cond-mat.mes-hall]
[35] Schwinger J 1951 *Phys. Rev.* **82** 664; Kim S P *et al* 2008 *Phys. Rev.* D **78**, 105013
[36] Rusin T M and Zawadzki W 2008 *Phys. Rev. B* **78** 125419; 2009 *B* **80** 045416; Vasko F T 2010 *Phys. Rev. B* **82** 245422
[37] Dawlati J M *et al* 2008 *Appl. Phys. Lett.* **98**, 0421161; Sun D *et al* 2008 *Phys. Rev. Lett.* **101** 157402 (2008).
[38] Singh V and Deshmukh M M 2009 *Phys. Rev.* B **80** 081404(R)
[39] Patanè D *et al* 2009 *Phys. Rev.* B **80** 024302
[40] Nair R R *et al* 2008 *Science* **320**, 1308 (2008); Mak K *et al* 2008 *Phys. Rev. Lett.* **101** 196405